Acta Biomaterialia 22 (2015) 141–154

Contents lists available at ScienceDirect

Acta Biomaterialia

journal homepage: www.elsevier.com/locate/actabiomat

Release and pharmacokinetics of near-infrared labeled albumin from monodisperse poly(D,L-lactic-*co*-hydroxymethyl glycolic acid) microspheres after subcapsular renal injection

F. Kazazi-Hyseni [a], S.H. van Vuuren [b], D.M. van der Giezen [b], E.H. Pieters [a], F. Ramazani [a], S. Rodriguez [c], G.J. Veldhuis [c], R. Goldschmeding [b], C.F. van Nostrum [a], W.E. Hennink [a], R.J. Kok [a,*]

[a] Department of Pharmaceutics, Utrecht Institute for Pharmaceutical Sciences (UIPS), Faculty of Science, Utrecht University, PO Box 80082, 3508 TB Utrecht, The Netherlands
[b] Department of Pathology, University Medical Center Utrecht, Heidelberglaan 100, 3584 CX Utrecht, The Netherlands
[c] Nanomi B.V., Zutphenstraat 51, 7575 EJ Oldenzaal, The Netherlands

ARTICLE INFO

Article history:
Received 20 December 2014
Received in revised form 25 March 2015
Accepted 21 April 2015
Available online 27 April 2015

Keywords:
Microspheres
Depot sustained release
Kidney
Near-infrared imaging
In vitro–in vivo correlation

ABSTRACT

Subcapsular renal injection is a novel administration method for local delivery of therapeutics for the treatment of kidney related diseases. The aim of this study was to investigate the feasibility of polymeric microspheres for sustained release of protein therapeutics in the kidney and study the subsequent redistribution of the released protein. For this purpose, monodisperse poly(D,L-lactic-*co*-hydroxymethyl glycolic acid) (PLHMGA) microspheres (40 μm in diameter) loaded with near-infrared dye-labeled bovine serum albumin (NIR-BSA) were prepared by a membrane emulsification method. Rats were injected with either free NIR-BSA or with NIR-BSA loaded microspheres (NIR-BSA-ms) and the pharmacokinetics of the released NIR-BSA was studied for 3 weeks by *ex vivo* imaging of organs and blood. Quantitative release data were obtained from kidney homogenates and possible metabolism of the protein was investigated by SDS–PAGE analysis of the samples. The *ex vivo* images showed a rapid decrease of the NIR signal within 24 h in kidneys injected with free NIR-BSA, while, importantly, the signal of the labeled protein was still visible at day 21 in kidneys injected with NIR-BSA-ms. SDS–PAGE analysis of the kidney homogenates showed that intact NIR-BSA was released from the microspheres. The locally released NIR-BSA drained to the systemic circulation and subsequently accumulated in the liver, where it was degraded and excreted renally. The *in vivo* release of NIR-BSA was calculated after extracting the protein from the remaining microspheres in kidney homogenates. The *in vivo* release rate was faster (89 ± 4% of the loading in 2 weeks) compared to the *in vitro* release of NIR-BSA (38 ± 1% in 2 weeks). In conclusion, PLHMGA microspheres injected under the kidney capsule provide a local depot from which a formulated protein is released over a prolonged time-period.

© 2015 Acta Materialia Inc. Published by Elsevier Ltd. All rights reserved.

1. Introduction

Acute kidney injury and chronic renal failure are conditions that are associated with high mortality rates [1–3]. These conditions often progress to end-stage renal failure and are characterized by the inability of the kidneys to adequately filter waste products from the blood [2]. One of the main causes for the progression toward renal failure is a local inflammatory process that occurs in the kidneys [2,4–6]. In this respect, several protein drugs are recognized as potential therapeutics for the treatment of renal diseases [7–10]. However, considering the pharmacokinetic characteristics of many proteins, including short half-life and instability, protein drugs require frequent administrations via injections [11]. The development of novel drug delivery systems, such as protein loaded polymeric microspheres, possibly overcomes the above mentioned shortcomings by encapsulation of the therapeutic and enabling its local and sustained release [12–14]. In addition, the local administration of a depot that affords continuous release of a therapeutic protein in the kidney may enable increased renal effectiveness combined with a reduction of extrarenal adverse effects. Subcapsular renal injection is a relatively new strategy for drug delivery to the kidney, where the drug eluting depot is injected with a small size needle under the kidney

* Corresponding author at: Department of Pharmaceutics, Utrecht Institute for Pharmaceutical Sciences, Universiteitsweg 99, 3584 CG Utrecht, The Netherlands. Tel.: +31 6 20275995.
E-mail address: r.j.kok@uu.nl (R.J. Kok).

http://dx.doi.org/10.1016/j.actbio.2015.04.030
1742-7061/© 2015 Acta Materialia Inc. Published by Elsevier Ltd. All rights reserved.

capsule. This technique has been recently studied for stem cells [15] and for drug eluting depots, i.e. hydrogels [16,17] and polymeric microspheres [18,19]. Dankers et al. [16] showed good biocompatibility of supramolecular hydrogels, suitable for short-time boost release of proteins, and demonstrated that a therapeutic protein (bone morphogenic protein 7) released from such a depot reduced local fibrotic responses in kidneys from healthy rats. Falke et al. [19] demonstrated that a depot of rapamycin-loaded microspheres inhibited fibrotic responses in rats with the unilateral ureter obstruction model. However, to our knowledge, there are no studies that report on the *in vivo* release profile and subsequent fate of the therapeutic compounds from such a subcapsular depot. Therefore, the purpose of the present study was to assess the feasibility of protein delivery from polymeric microspheres that have been injected subcapsularly, as well as the subsequent fate after intrarenal delivery.

The applied microspheres in this study were based on poly(D,L-lactic-*co*-hydroxymethyl glycolic acid) (PLHMGA), an aliphatic polyester with improved properties for protein delivery [20–23]. Recently, it was demonstrated that monodisperse PLHMGA microspheres have good biocompatibility after subcutaneous and subcapsular renal administration in rats [18]. Such monodisperse microspheres can be prepared by membrane emulsification method, in which uniform-sized droplets are formed after a primary W/O emulsion (containing protein and polymer solutions, respectively) is pressed through a membrane with uniformly sized pores [24,25]. In the present study, PLHMGA microspheres were loaded with near-infrared (NIR) dye labeled albumin (NIR-BSA). The advantage of labeling proteins with NIR dyes is that the NIR wavelength (700–900 nm) ensures sensitive detection of the labeled protein, as living tissues have relatively low absorbance and scattering in this range [26]. One of the major challenges, however, is to discriminate between NIR signal of NIR-BSA that is still loaded in the polymeric microspheres and the NIR-BSA released from the microspheres. The latter can be either intact or metabolically processed by the kidney. Therefore, at different time points after injection, animals were sacrificed and the levels of released NIR-BSA were quantified in kidney homogenates. This approach provides valuable data about the release of the model protein from the microspheres injected under the renal capsule as well as pharmacokinetic data that can be used to predict the further pharmacokinetic fate of proteins once released in the kidney parenchyma.

2. Materials and methods

2.1. Materials

O-Benzyl-L-serine was purchased from Senn Chemicals AG (Dielsdorf, Switzerland). D,L-lactide was purchased from Purac (The Netherlands). Tin(II) 2-ethylhexanoate ($SnOct_2$), poly(vinyl alcohol) (PVA; M_w = 13,000–23,000), dimethylsulfoxide (DMSO) and bovine serum albumin (BSA; A4503) with molecular weight of 66,776 Da, were obtained from Sigma–Aldrich (Germany). 1,4-Butanediol 99 + % was obtained from Acros Organics (Belgium). IRDye® 800CW – NHS ester (MW = 1166 Da) from LI-COR Biosciences was supplied by Westburg BV (Leusden, The Netherlands). Carboxymethyl cellulose (CMC, with viscosity of 2000 mPa·s of a 1% solution in water) was obtained from Bufa B.V. (255611, The Netherlands). Halt™ Protease and phosphatase inhibitor cocktail, EDTA-free (78445) was obtained from Thermo Scientific (IL, USA). RIPA buffer (50 mM Tris–HCl, pH 7.5, 150 mM sodium chloride, 1% Triton X-100, 1% sodium deoxycholate, 0.1% SDS, 2 mM EDTA) was provided by Teknova (CA, USA). Sodium phosphate dibasic (Na_2HPO_4) and sodium azide (NaN_3) were purchased from Fluka (The Netherlands). Dichloromethane (DCM), chloroform, tetrahydrofuran and methanol were purchased from Biosolve BV (The Netherlands). Sodium dihydrogen phosphate (NaH_2PO_4) and sodium chloride (NaCl) were supplied from Merck (Germany).

2.2. Methods

2.2.1. Synthesis and characterization of PLHMGA

Poly(D,L-lactic-*co*-hydroxymethyl glycolic acid) (PLHMGA) was synthesized as previously described by Leemhuis et al. [27]. In this study, a molar ratio of 35% BMMG (3*S*-(benzyloxymethyl)-6*S*-methyl-1,4-dioxane-2,5-dione) and 65% D,L-lactide (mol/mol) was used, with butanediol as an initiator (1:300 mol/mol monomer) and tin (II) 2-ethylhexanoate as a catalyst (1:600 mol/mol monomer). Molecular weight of PLHMGA was determined by GPC (Waters Alliance System) using a Waters 2695 separating module and a Waters 2414 refractive index detector, operating with tetrahydrofuran at a flow rate of 1 mL/min, and calibrated with polystyrene standards (PS-2, M_w = 580–377,400 D, EasiCal, Varian). Two PL-gel 5 μm Mixed-D columns fitted with a guard column were used. The copolymer composition was determined with NMR (Gemini-300 MHz) analysis, using chloroform-d, 99.8 atom% (Sigma–Aldrich) as solvent. The thermal properties of the copolymer were measured with differential scanning calorimetry (DSC – Q 2000, TA Instruments). For DSC measurements, approximately 5 mg of the copolymer was placed in aluminum pan (T zero pan/lid set, TA Instruments) and the sample was scanned with a modulated heating method in three cycles [20]. The sample was heated until 120 °C (5 °C/min) and then cooled down to −50 °C, followed by a heating until 120 °C (5 °C/min). The temperature modulation was ±1 °C/min.

2.2.2. Conjugation of NIR dye to BSA

The NIR dye, IRDye® 800CW – NHS ester, was conjugated to BSA following the manufacturer's protocol for labeling high molecular weight proteins (LI-COR, Inc. Biosciences). In brief, BSA dissolved in water (10 mg/ml) was brought to pH 8.5 with 1 M potassium phosphate (pH 9) and mixed with a solution of the dye (4 mg/ml DMSO) in a 3:1 dye:BSA mol/mol ratio. The albumin/dye solution was incubated for 2 h at room temperature while gently stirred and protected from light. The labeled protein was purified by size exclusion chromatography with Zeba™ desalting Spin Columns (Thermo Scientific), yielding a buffer salt-free protein solution that was freeze-dried (Alpha 1–2, Martin Christ, Germany). The lyophilized protein was kept in −20 °C until further use. The purity of NIR-BSA was analyzed with GPC (Waters Alliance System) using a Waters 2695 separating module and a Waters photodiode array, with PBS as an eluent and at a flow rate of 1 mL/min. The column used was Biosep-3000 (Phenomenex, Germany). The dye-to-protein ratio of the conjugate was determined according to the manufacturer's protocol (LI-COR, Inc. Biosciences) by measuring the absorbance of NIR-BSA at 280 and 780 nm with a UV spectrophotometer (UV-2450 Shimadzu, Japan). The conjugate was diluted in a mixture of PBS and methanol (1:1) and the following formula was used for calculating the dye/protein (D/P in mol/mol) ratio,

$$D/P = \left[\frac{A_{780}}{\varepsilon_{\text{dye}}}\right] \div \left[\frac{A_{280} - (0.03 \times A_{780})}{\varepsilon_{\text{protein}}}\right]$$

where 0.03 is a correction factor for the absorbance of the IRDye® 800CW at 280 nm (equal to 3.0% of its absorbance at 780 nm) while ε_{dye} (270,000 $M^{-1}\,cm^{-1}$; LI-COR Biosciences) and $\varepsilon_{\text{protein}}$ (43,824 $M^{-1}\,cm^{-1}$ [28]) are molar extinction coefficients for the dye and BSA, respectively.

A

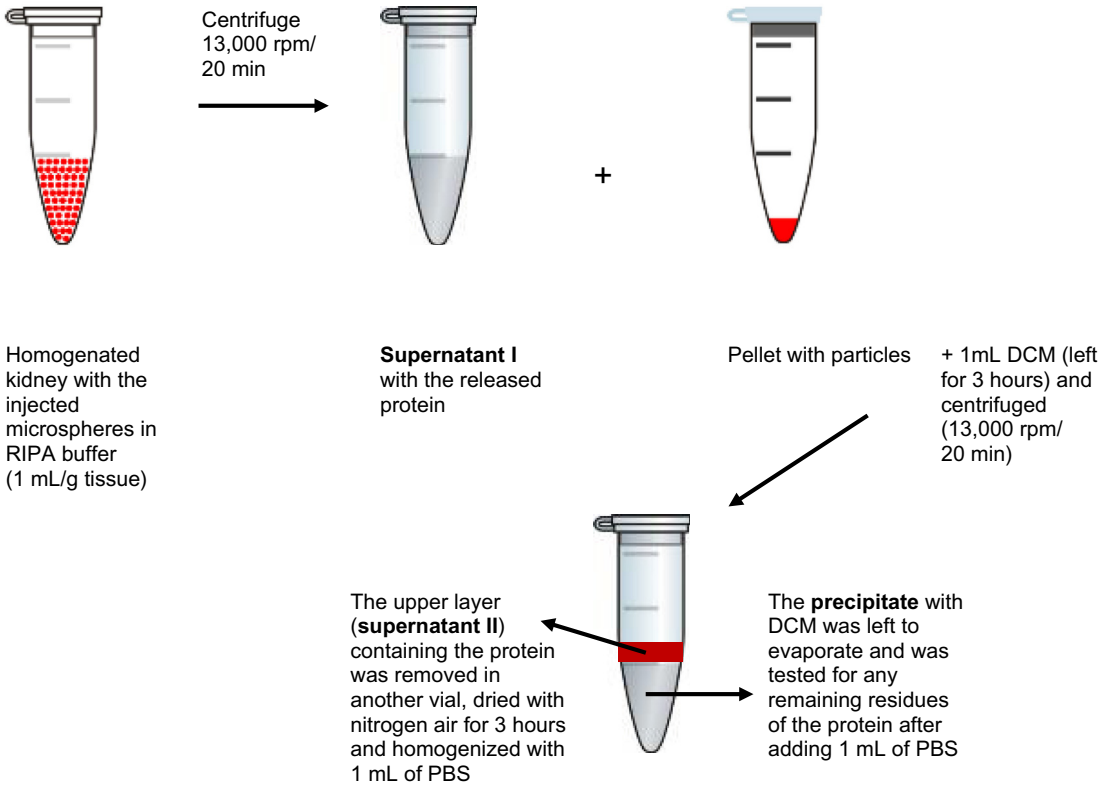

B

Kidney homogenate spiked with:	Amount of NIR-BSA (mg/mL)	Supernatant I (%)	Supernatant II (%)	Precipitate (%)	Recovery (%)
Free NIR-BSA	1.0	100 ± 1	2.0 ± 0.1	0.24 ± 0.01	102 ± 1
NIR-BSA-ms	0.3	12 ± 1	62 ± 5	0.36 ± 0.05	74 ± 4

Fig. 1. (A) The extraction method of NIR-BSA from homogenates of left kidneys injected with NIR-BSA microspheres to determine the released protein from the microspheres (supernatant I) and protein loaded in the microspheres (supernatant II). (B) Results of the optimization of the extraction procedure. For optimization, kidney homogenates were spiked with either empty microspheres and known amount of free NIR-BSA ($n = 2$) or with NIR-BSA loaded microspheres ($n = 3$).

2.2.3. Preparation and characterization of NIR-BSA loaded PLHMGA microspheres

PLHMGA microspheres were prepared with a cross-flow membrane emulsification process, where the dispersed phase (W_1/O) was pumped into the continuous phase (W_2) which was flowing along the membrane (hydrophilic Iris-20, microsieve™ membrane technology, Nanomi B.V., The Netherlands) [24,29]. The dispersed phase (W_1/O) was prepared by adding 0.8 mL of a solution containing BSA and NIR-BSA in water (1:1; 50 mg protein/ml) to 20% w/w PLHMGA in DCM solution (1.1 g PLHMGA/3.24 mL DCM). The dispersed phase was homogenized using an Ultra-Turrax T8 (IKA Works, USA) with dispersing element S10N-10G, at a speed of 20,000 rpm for 30 s. Next, the dispersed phase was passed through the Iris-20 membrane at a constant rate of 10 mL/h using a syringe pump (Nexus 6000, Chemyx, USA) into 60 mL of the continuous phase (PVA 4% in water, w/v). The continuous phase was pumped with a rate of 4.6 mL/min across the membrane. At the end of the process (24 min), the formed emulsion was stirred for 3 h to evaporate DCM. The hardened microspheres were collected by centrifugation at 3000 rpm for 2 min (Hermle Z233MK-2 centrifuge), washed three times with water, frozen with liquid nitrogen and freeze-dried (Alpha 1–2, Martin Christ, Germany). Blank PLHMGA microspheres were prepared with the same procedure, except that the internal water phase (W_1) contained no protein. All the particles were prepared aseptically in a flow cabinet using autoclaved equipment and sterile water.

The volume-weight mean diameter of the obtained microspheres was measured with an optical particle sizer (Accusizer 780, Santa Barbara, California, USA). At least 5,000 microspheres were analyzed. The BSA loading content of the microspheres was determined by dissolving 10 mg of microspheres in 1 mL of DMSO for one hour followed by the addition of 5 mL of 0.05 M NaOH and 0.5% SDS solution [20,30]. The BSA concentration of the formed solution was measured with BCA protein assay (Interchim, USA) according to the manufacturer's protocol. The loading efficiency was calculated as the amount of BSA entrapped in the microspheres divided by the BSA amount added during the preparation of microspheres, times 100%. The loading of NIR-BSA

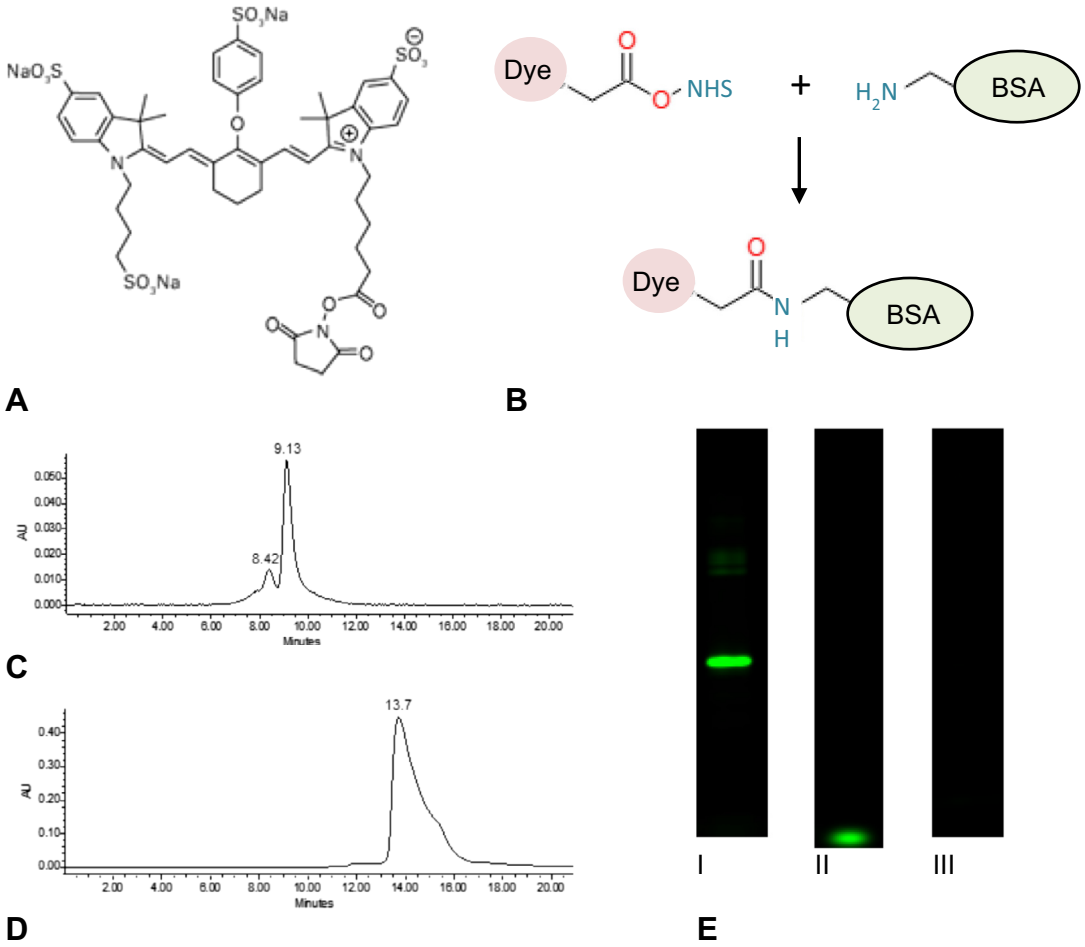

Fig. 2. Labeling of bovine serum albumin (BSA) with NIR dye and analysis of the purity of the labeled NIR-BSA. (A) Structure of the NIR dye (IRDye® 800CW NHS ester); (B) reaction between the NIR dye and BSA; (C) GPC chromatogram of NIR-BSA detected at 780 nm; (D) GPC chromatogram of the NIR dye detected at 780 nm; (E) SDS–PAGE gels imaged with Odyssey near-infrared imager ((I) NIR-BSA; (II) NIR dye and (III) Unlabeled BSA).

was not measured with an infrared imager as the NIR signal was lost after the addition of NaOH to the solution (results not shown). Bjornson et al. [31] also reported that the half-life of another near-infrared dye, indocyanin green, in alkaline solution was only 2 h as a result of the formation of basic colorless compounds when this dye was exposed to alkaline solutions.

2.2.4. In vitro degradation and release study of PLHMGA microspheres

Around 10 mg of NIR-BSA encapsulated PLHMGA microspheres (NIR-BSA-ms) was suspended in 1.5 mL of 100 mM phosphate buffer (pH 7.4) containing 56 mM NaCl, 33 mM NaH_2PO_4, 66 mM Na_2HPO_4 and 0.05% (w/v) NaN_3 (to prevent bacterial growth). The vials, protected from light, were incubated at 37 °C while gently shaking. At different time-points, a single sample of NIR-BSA microspheres was analyzed for polymer degradation, while triplicate samples were analyzed for NIR-BSA release. To study polymer degradation, the sample was centrifuged (4000 rpm for 5 min; Hermle Z233MK-2 centrifuge), after which the pellet was washed three times with water, lyophilized and analyzed for residual dry weight and PLHMGA molecular weight, as described in Section 2.2.1. For analysis of NIR-BSA at indicated time-points, three vials were centrifuged and the supernatant was removed, replaced by fresh release buffer and the vials were placed back in the incubator. The amount of released protein was measured in the supernatant by BCA protein assay, whereas the release of NIR-BSA was also quantified with Odyssey near-infrared scanner (LI-COR, Inc. Biosciences) employing a 800 nm detector. Calibration was done with NIR-BSA dissolved in the release buffer with concentration ranging from 0.008 to 17 μg/mL for the Odyssey imager, whereas for the BCA protein assay BSA was used in concentrations ranging from 10 to 100 μg/mL.

2.2.5. Animal experiments

The protocol for the animal experiments was approved by the Animal Ethics Committee of the University of Utrecht (Number 2012.II.09.133). The animal experiments were carried out using female Fischer 344 rats (Harlan Nederland, The Netherlands) with an average weight of 170 g. Animals had free access to acidified water and standard laboratory chow, and were housed according to institutional rules with 12:12 h dark/light cycles. Rats were anesthetized by inhalation of isoflurane (4% induction, 1.5–3% for maintenance of anesthesia) and were given carprofen (5 mg/kg s.c.) analgesia at 12 h and 24 h after the surgical intervention. The left kidney was exposed by a retroperitoneal incision and gently lifted to allow the injection of the samples under the renal capsule. To this end, two adjacent pockets were created under the renal capsule with a 26G blunt Hamilton needle (Chrom8 International, the Netherlands) and 25 μL of the sample was injected in each pocket with the same needle (50 μL per kidney). The injection spot in the renal capsule was sealed with fibrin glue (Tissucol® DUO 500, Baxter AG, Austria) to prevent reflux of the

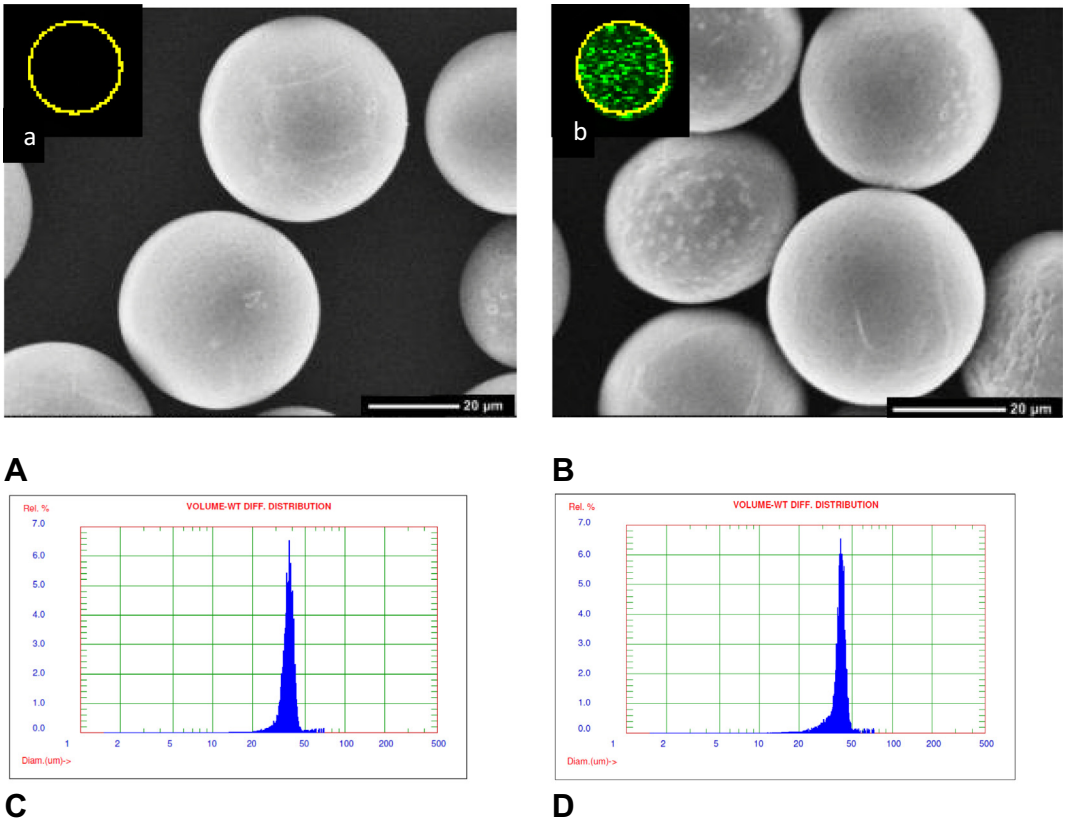

Fig. 3. Characteristics of PLHMGA microspheres. (A, a and C) blank PLHMGA microspheres; (B, b and D) NIR-BSA loaded PLHMGA microspheres. (A, B) Representative SEM photographs (magnification ~1000×); (a, b) visualization of microspheres with Odyssey near-infrared imager (the yellow line is the circumference of a single well of a 96-well plate) and (C, D) volume weight particle diameter distribution as measured with AccuSizer.

injected fluid upon withdrawal of the needle from the subcapsular pocket.

Animals were divided into three groups. The rats of the first group ($n = 15$, 3 animals per time-point) were injected with 50 µL of a dispersion of NIR-BSA-ms in vehicle (10 mg microspheres/50 µL, equivalent to 160 µg NIR-BSA; composition of vehicle see below). Rats of the second group ($n = 5$, 1 animal per time-point) were injected similarly with 50 µL of a dispersion of placebo microspheres, while rats of the third group ($n = 15$, 3 animals per time-point) were injected with a solution of 160 µg NIR-BSA in 50 µL vehicle. Vehicle for the injections was a solution of 0.6% carboxymethyl cellulose containing 0.02% Tween-20 and 5% mannitol, which was autoclaved before dispersion of the microspheres or dissolution of NIR-BSA. Animals from the first and the second group (i.e. rats injected with microspheres) were sacrificed at day 0 (directly after injection) and at day 3, 7, 14 and 21 post injection. Rats injected with NIR-BSA were sacrificed at 0, 2, 4, 6 and 24 h post injection. Animals were anesthetized and a blood sample from the aorta was collected in EDTA tubes. Heart, lungs, spleen, kidneys, liver and bladder were excised, snap frozen with liquid nitrogen and kept in −20 °C until further measurements. From the rats of the first group (i.e. NIR-BSA-ms group) blood samples were also harvested, via the tail vein, in between the sacrificing time-points (0, 2, 4, 6, 24 h and at every other day until 21 days).

2.2.6. NIR imaging of kidneys and other organs

The strength of the NIR signal in the collected organs was imaged by scanning of the excised organs with an Odyssey scanner at the 800 nm filter. Prior to imaging, the kidneys and other organs were defrosted and rinsed with saline. Kidneys were cleaned from the surrounding fat tissue. A region of interest encompassing the whole organ was scanned and reported as relative fluorescence values calculated by the manufacturer's software. The background signal was corrected by scanning the representative organs of animals injected with blank microspheres.

2.2.7. Analysis of NIR fluorescence in blood

Blood samples were serially diluted (1:2 dilution steps) in 96-well plates with RIPA buffer (supplemented with protease and phosphatase inhibitor cocktail). The serial dilutions were made to determine the range where the fluorescence intensity varies in a linear manner with the concentration, to avoid saturation of the fluorescent signal [32]. NIR fluorescence was determined by scanning with an Odyssey scanner. Only values in the linear range were used to calculate the relative fluorescence in blood. Calibration curves were made by spiking blood from control rats with NIR-BSA (range 0.008–17 µg/mL).

Blood samples were also subjected to SDS–PAGE electrophoresis followed by NIR scanning of the gels, in order to discriminate NIR fluorescent degradation products from intact NIR-BSA (NuPAGE® Novex® 4–12% Bis–Tris gels, non-reducing conditions). As a control, NIR-BSA (10 µg/mL) and NIR dye (0.5 µg/mL) were used. After separation, the gels were visualized with Odyssey imager. The detection limit of NIR-BSA with this method was 0.6 µg/mL.

2.2.8. Analysis of NIR fluorescence in tissue homogenates

Organs were mixed with RIPA buffer supplemented with protease and phosphatase inhibitors (1 mL of buffer/g of tissue) in tissue homogenizing tubes containing zirconium oxide beads (Tissue homogenizing CK28 – 2 or 7 mL, Bertin technologies, France) and

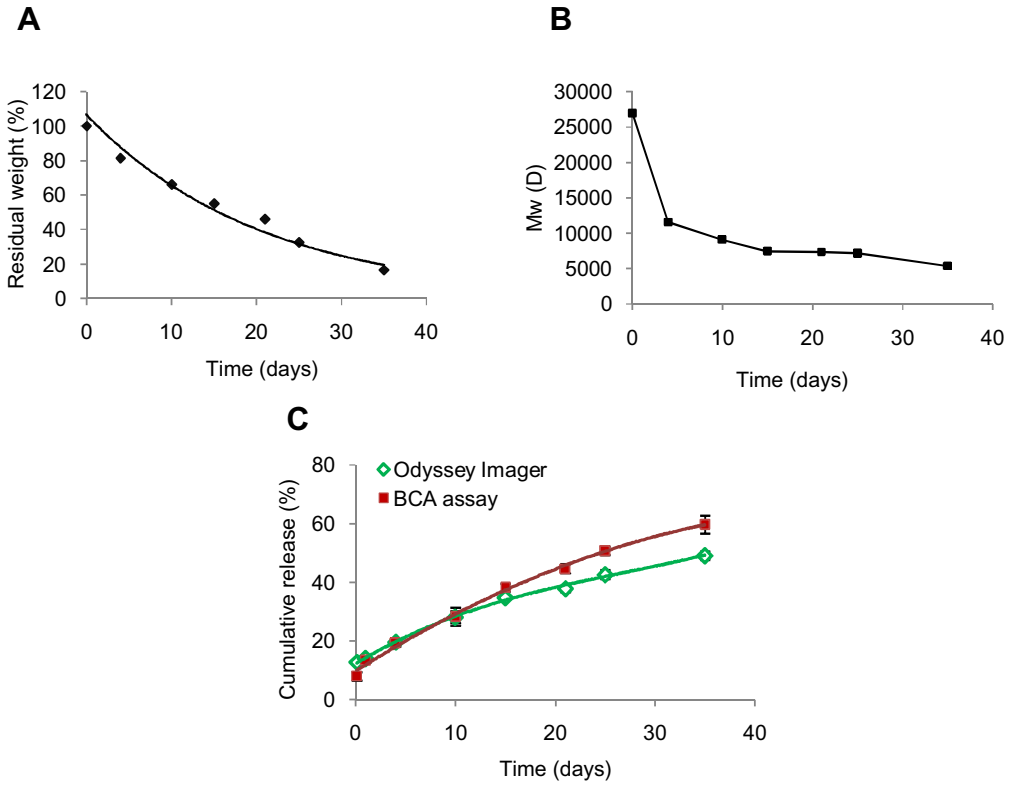

Fig. 4. *In vitro* degradation of NIR-BSA loaded PLHMGA microspheres and the cumulative release profile of protein over time: (A) Residual weight of the microspheres (%) ($n = 1$), (B) PLHMGA weight average molecular weight (M_w) ($n = 1$) and (C) Cumulative release of NIR-BSA and BSA from PLHMGA microspheres in PBS measured with Odyssey infrared imager (NIR-BSA release) and with BCA assay (total BSA release) ($n = 3$).

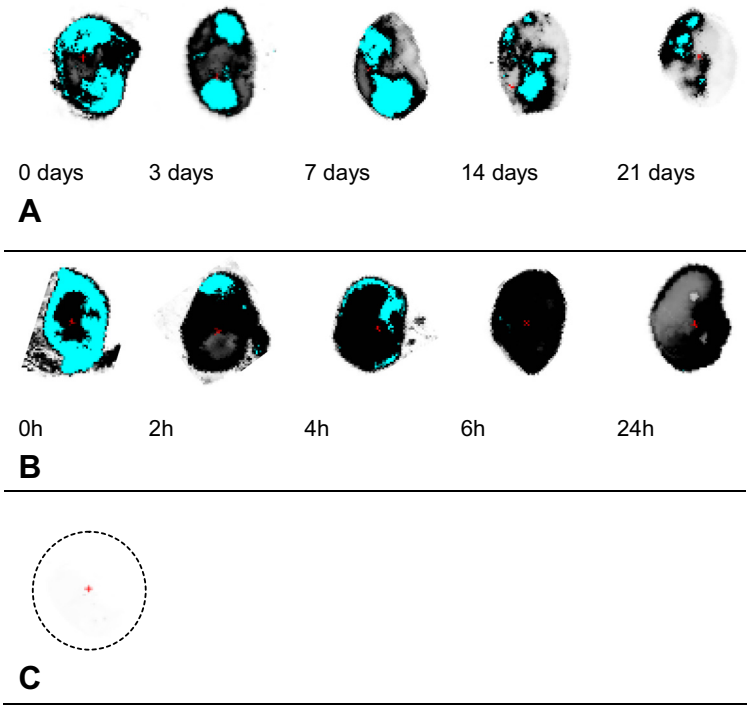

Fig. 5. NIR-imaging of the injected kidneys visualized *ex vivo* with Odyssey infrared imager. (A) Images of kidneys injected with NIR-BSA microspheres explanted at time points up to 3 weeks post injection. (B) Images of kidneys injected with free NIR-BSA explanted at time points up to 24 h post injection. (C) Blank kidney from the control group showing no fluorescence signal. Colors from gray to black represent the signal of the NIR dye from low to high signal, respectively. Cyan color indicates overexposure of the fluorescent signal.

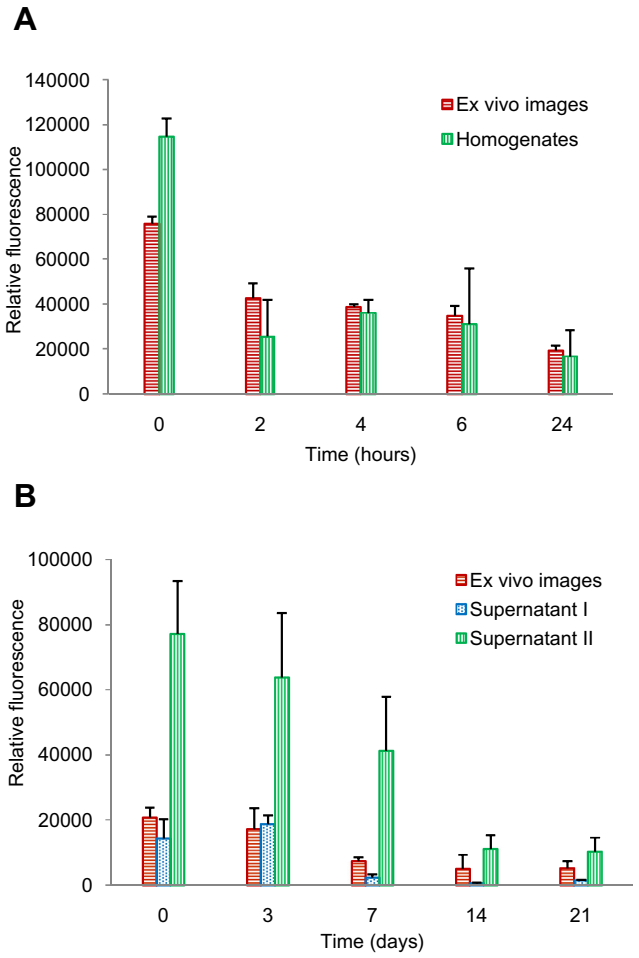

Fig. 6. Relative fluorescence of the left kidneys ($n = 3$) injected with (A) NIR-BSA and (B) NIR-BSA microspheres. Homogenates of the kidneys injected with NIR-BSA microspheres were treated according to the procedure described in Fig. 1A, where supernatant I refers to the released NIR-BSA and supernatant II refers to NIR-BSA recovered from the implanted microspheres.

homogenized at a speed of 4000 rpm for 5 s (Precellys24 tissue homogenizer, Bertin technologies, France). All tissue homogenates were also analyzed by SDS–PAGE as described in Section 2.2.7. Homogenates of the left kidneys injected with free NIR-BSA were further analyzed for quantitative measurements of the NIR fluorescence after serial dilutions, as described in Section 2.2.7. Homogenates of the left kidneys injected with NIR-BSA-ms were extracted as shown in Fig. 1A, in order to differentiate between released NIR-BSA and NIR-BSA still entrapped in the microspheres. In brief, the left kidney homogenates in RIPA buffer were centrifuged (13,000 rpm for 20 min; Hermle Z233MK-2 centrifuge) and the supernatant containing the released NIR-BSA (supernatant I) was harvested. The pellet with kidney tissue and the injected microspheres was treated with 1 mL of DCM while gently shaking for 3 h to fully dissolve the microspheres, and centrifuged. NIR imaging of the sample confirmed that the protein from the microsphere pellet was now in the layer floating on top of the DCM layer. This upper layer (supernatant II) was carefully transferred into another vial. The remaining traces of DCM were evaporated under nitrogen gas and the samples were homogenized with 1 mL of PBS. Both supernatants were serially diluted in 96-well plates and measured with Odyssey imager. For calibration, NIR-BSA in RIPA buffer was used for supernatant I and NIR-BSA in PBS for supernatant II. The method was optimized by spiking control kidney homogenates with a known amount of NIR-BSA loaded microspheres (Fig. 1B).

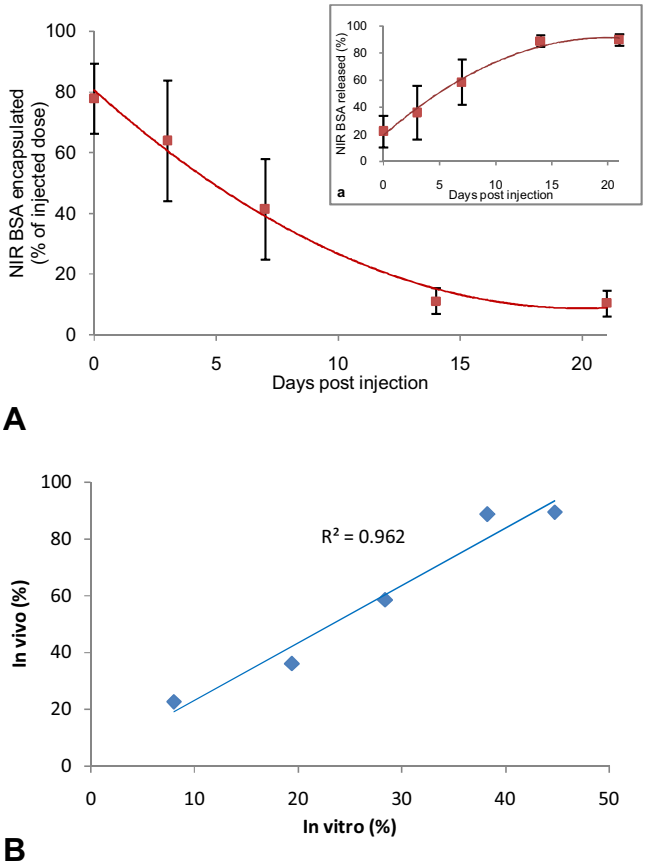

Fig. 7. Analysis of NIR-BSA release from a subcapsular microsphere depot over time. (A) NIR-BSA extracted from microspheres was measured as outlined in Fig. 1A (supernatant II), and expressed as percentage of the injected dose of NIR-BSA; insert (a) *in vivo* cumulative release of NIR-BSA. (B) *In vitro–in vivo* correlation plot of NIR-BSA release. The fitted linear curve showed an R^2 of 0.96.

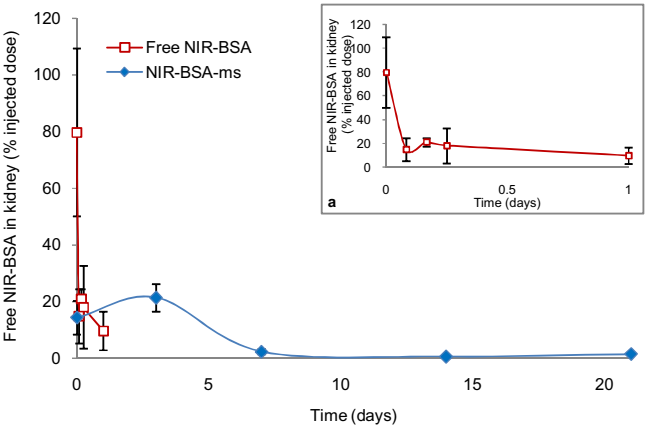

Fig. 8. Free/released NIR-BSA measured in the kidney homogenates ($n = 3$) injected subcapsularly with NIR-BSA (also shown in a) or with NIR-BSA microspheres. NIR-BSA levels were determined as shown in Fig. 1A (supernatant I) and expressed as the percentage of the injected dose of NIR-BSA.

2.2.9. Calculations and statistical analysis

The *in vivo* cumulative release of NIR-BSA from kidneys injected with NIR-BSA-ms was calculated as 100 – percentage of NIR-BSA recovered from the injected microspheres. The *in vitro–in vivo* level A correlation curve was plotted as the percentage of the released

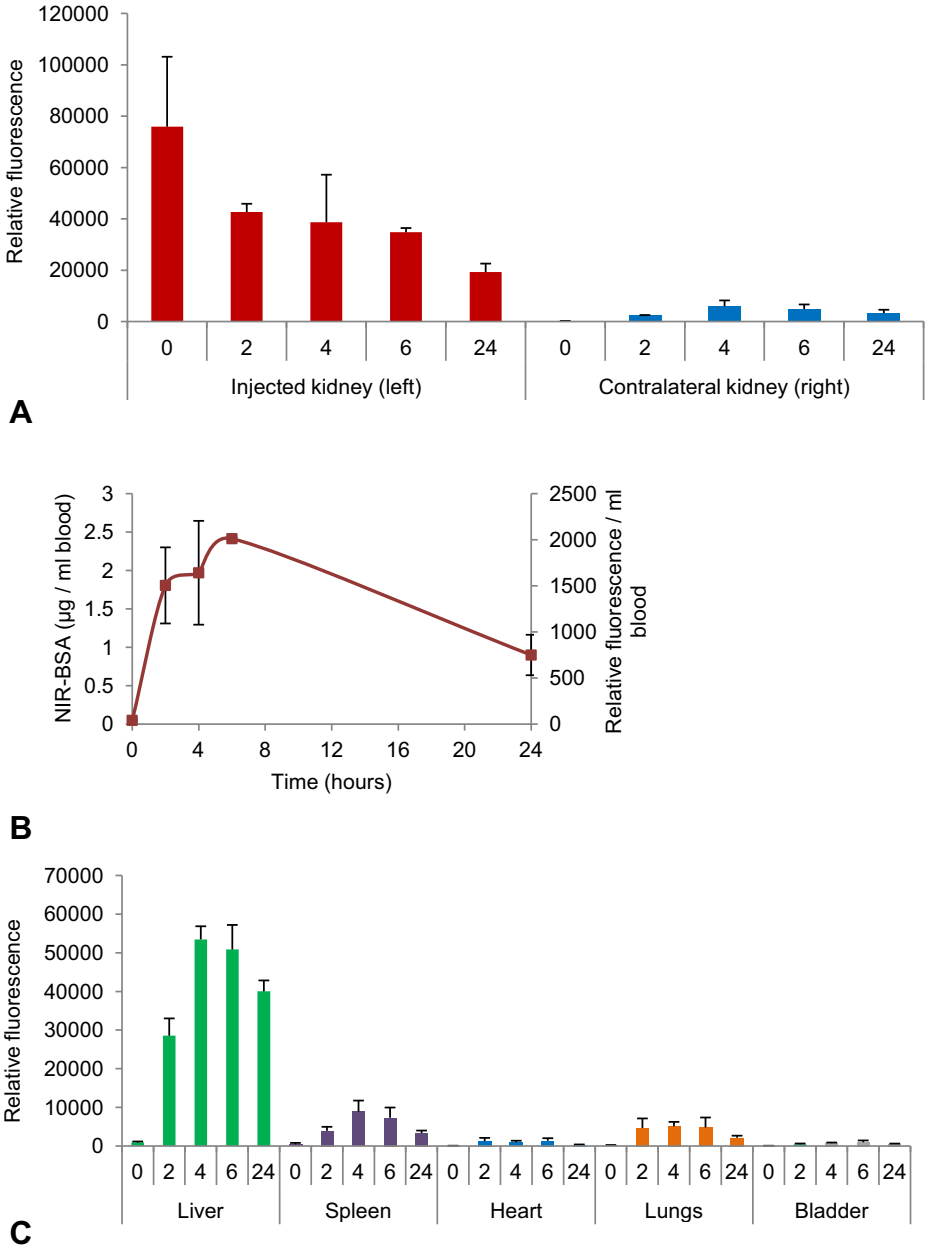

Fig. 9. Biodistribution of NIR-fluorescent compounds in animals injected with NIR-BSA ($n = 3$). Organs were explanted and blood samples were collected at time 0, 2, 4, 6 and 24 h and were imaged with Odyssey infrared imager. (A) Injected left kidney and the contralateral kidney, (B) Blood samples and (C) Other organs (liver, spleen, heart, lungs and bladder which also contained urine).

NIR-BSA *in vitro* (measured with the BCA assay) versus the percentage of NIR-BSA released *in vivo*, as shown elsewhere [33,34]. NIR-BSA concentrations measured in the injected left kidneys (supernatant I) were used to calculate the renal area under the curve (AUC) by the trapezoidal rule. All data are represented as mean ± standard deviation.

3. Results and discussion

3.1. Labeling of BSA and preparation of PLHMGA microspheres

Near infrared (NIR) dye (IRdye® 800CW-NHS) was conjugated to BSA (MW 66 kDa) with an average of 1.3 molecules of NIR dye per molecule of BSA (Fig. 2A and B). GPC and SDS–PAGE analysis of purified NIR-BSA demonstrated that free dye could not be detected in the product and no aggregates of BSA were visible (Fig. 2C–E). PLHMGA with weight average molecular weight (M_w) of 27 kD, polydispersity of 1.8 and glass transition temperature of 35 °C, was used to prepare NIR-BSA loaded microspheres (NIR-BSA-ms) by cross-flow membrane emulsification process, which yielded monodisperse microspheres with a smooth surface and no visible pores (Fig. 3A and B). NIR-BSA-ms had a volume weight mean diameter of 40 ± 5 µm, while blank microspheres had a mean diameter of 37 ± 4 µm (Fig. 3C and D). The BSA loading was 31 mg/g polymer (theoretical albumin loading was 36 mg/g) and the loading efficiency was 87%. Fig. 4(A and B) shows the results of the *in vitro* degradation of the microspheres at 37 °C. PLHMGA microspheres loaded with NIR-BSA showed a continuous weight loss and a decrease in weight average molecular weight (M_w) during the course of the 35-day incubation, suggesting degradation via bulk erosion [35,36]. The observed erosion rate is similar to the degradation of empty PLHMGA microspheres with same size

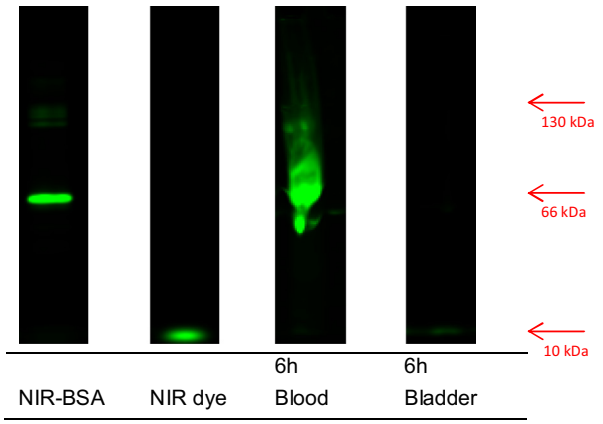

Fig. 10a. SDS–PAGE analysis of reference compounds NIR-BSA, NIR dye, blood and bladder homogenate of animals injected with NIR-BSA. Rats were sacrificed at 0, 2, 4, 6 and 24 h after injection. The blood sample and bladder homogenate are shown at time point 6 h after injection, when the detected fluorescent signal was the highest in these samples. No signal was detected at other time-points.

and polymer composition [18]. The *in vitro* cumulative protein release from microspheres, determined both with the NIR imager and the BCA protein assay, was comparable for the two methods (Fig. 4C). During the course of the incubation of 35 days, after a burst release of 8 ± 1% (within 3 h of incubation), around 60 ± 3% of the encapsulated protein was released from the PLHMGA microspheres, in agreement with the results of a previous study [20]. A slightly lower total recovery of NIR-BSA was determined by NIR analysis compared to the cumulative recovery by BCA protein analysis (Fig. 4C). A plausible explanation for this might be the instability of the dye at 37 °C, which was also observed when NIR-BSA was incubated in buffer for a period of one month.

3.2. Ex vivo imaging of subcapsularly injected depots

Since normal tissues do not absorb NIR light extensively, NIR optical imaging is emerging as an alternative to radiotracer-based scanning techniques for studying the pharmacokinetics of (bio)macromolecules and drug delivery systems [37–40]. In animal studies, NIR *in vivo* imaging is now regularly

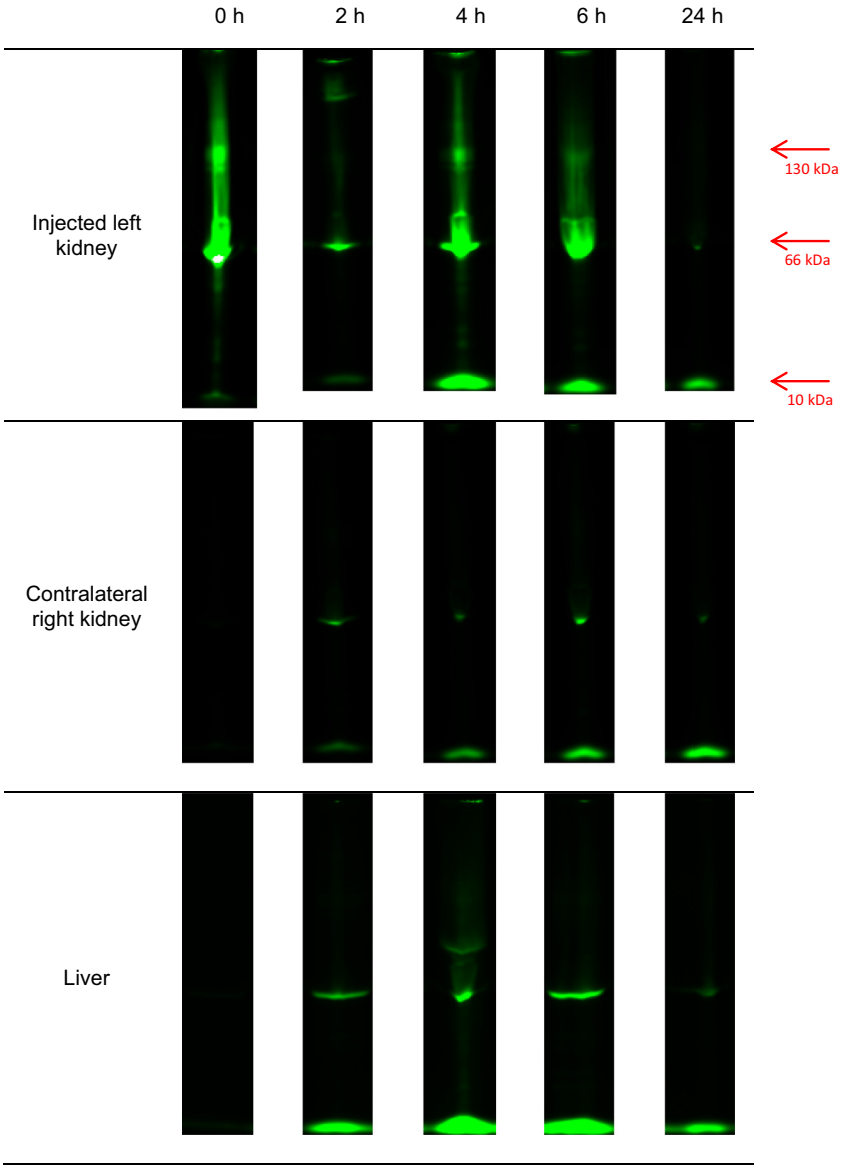

Fig. 10b. SDS–PAGE analysis of organ homogenates from animals injected with NIR-BSA. The animals were sacrificed at 0, 2, 4, 6 and 24 h after injection.

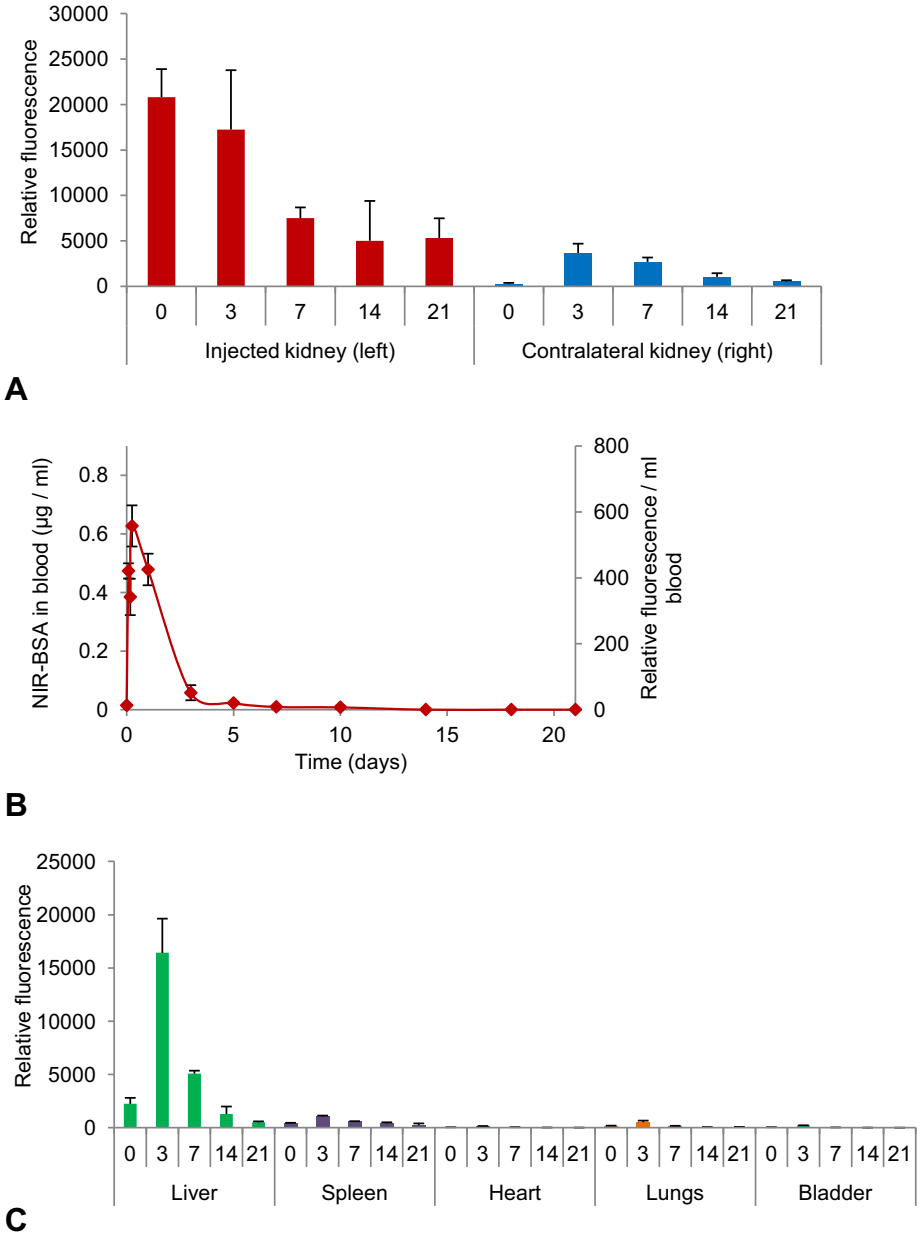

Fig. 11. Biodistribution of NIR-fluorescent compounds in animals injected with NIR-BSA microspheres ($n = 3$). Organs were explanted at day 0, 3, 7, 14 and 21 and were imaged with Odyssey infrared imager. Blood samples were collected also in between time-points. (A) Injected left kidney and contralateral right kidney, (B) Blood samples (signal detected until day 10 after injection) and (C) Other organs (liver, spleen, heart, lungs and bladder which also contained urine).

applied for monitoring the tumor accumulation of nanoparticles or other types of nanocarriers, especially in subcutaneously implanted tumor xenografts [41,42]. Major limitations of *in vivo* imaging are, however, the proper visualization of fluorescence accumulation in organs in the peritoneal cavity due to scattering of the emitted light [43] and thus quantification of the obtained signals [32]. It has been shown that better imaging results, from magnetic resonance imaging, can be obtained when the kidney is repositioned to a more superficial location in the abdomen [44]. Such an invasive surgical procedure will, however, also affect the normal perfusion and physiological function of the kidney. Other studies also report quantification of the signal in whole body imaging with non-invasive tomographic imaging [42,45]. However, these techniques are relying on mathematical algorithms to compensate for scattering of the signal [42,45]. Moreover, in this study, we also aimed to differentiate between the NIR signal from released NIR-BSA and the protein still loaded in the microspheres. Therefore, we proceeded with *ex vivo* imaging of the organs and analysis of the NIR signal in kidney homogenates as described below.

The kidneys injected with NIR-BSA and with NIR-BSA-ms were imaged *ex vivo* after termination of the animals. In Fig. 5A it is shown that kidneys injected with NIR-BSA-ms contained two adjacent pockets filled with the implanted microspheres, which can be explained by the applied injection procedure as described in Section 2.2.5. The NIR signal in the kidneys of the animals of this group decayed reaching around 20% intensity of the signal at the end of the experiment. These data suggest that PLHMGA microspheres injected under the kidney capsule degrade over time while continuously releasing the encapsulated NIR-BSA protein. Fig. 5B shows the images of kidneys injected with NIR-BSA, i.e. the labeled protein dissolved in the viscous vehicle. As can be observed, the

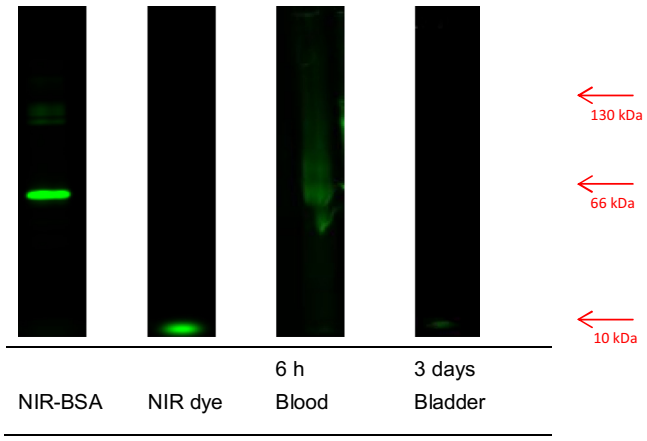

Fig. 12a. SDS–PAGE of reference compounds NIR-BSA, NIR dye and blood and bladder homogenate of animals injected with NIR-BSA microspheres. The animals were sacrificed at day 0, 3, 7, 14 and 21. Blood samples were collected additionally in between time-points. The blood sample and bladder homogenate are shown at time-point 6 h and 3 days, respectively, the time-points with maximum detected concentration. There is a faint band present in the blood sample at 66 kDa and in the bladder homogenate at 10 kDa. No signal was detected in blood and bladder samples at other time-points.

injected protein was distributed throughout the kidney showing a widespread fluorescence as a result of fluid convection under the renal capsule. The fluorescent signal decreased gradually afterward, resulting in relative low fluorescence intensity levels at 24 h post injection. The relative fluorescence at this time-point was, however, higher than the background signal of blank kidney, as can be observed in Fig. 5C. These data support that the protein released from the microspheres is able to distribute further over the kidney and, in principle, can also reach more distant areas in this organ. Furthermore, the disappearance of locally injected NIR-BSA within hours after its injection also underscores the need for a depot system that can effectuate prolonged levels of the released protein in the kidney.

3.3. Quantification of NIR-BSA in kidney homogenates

To quantify the levels of NIR-BSA, the injected kidneys were homogenized and analyzed with an Odyssey infrared imager, after serial dilution of the homogenates. The serial dilutions are necessary to obtain samples that are in the linear range of the fluorescence detection to avoid underestimation of the signal as a result of saturation [32]. Homogenates of the kidneys injected with NIR-BSA-ms were further treated with the method shown and described in Fig. 1A, where the released protein was separated from the protein still encapsulated in the microspheres. In the homogenized kidney tissues spiked with NIR-BSA-ms (Fig. 1B), this extraction method showed a total NIR-BSA recovery of 62 ± 5 % from the extracted pellet (supernatant II) and an additional 12 ± 1% of NIR-BSA released directly in supernatant of the homogenized tissue (supernatant I). The initial release after tissue homogenization is in good agreement with the results of the *in vitro* burst release of NIR-BSA-ms (Fig. 4C). These results show that the quantification of NIR-BSA levels within tissue and its further subdivision in encapsulated and released protein is only semi-quantitative, as it was not further corrected or normalized for the recovery of the extraction method. Nevertheless, as shown in Fig. 6, NIR fluorescence quantification was more accurate in homogenized tissues compared to image analysis of the *ex vivo* scanned kidneys. For rats injected with NIR-BSA (Fig. 6A) a large difference was observed at the first time-point, immediately after injection. This can be explained by oversaturation and quenching of the NIR signal in the *ex vivo* imaging analysis, which was overcome by diluting the homogenate samples. Moreover, in kidneys injected with NIR-BSA-ms (Fig. 6B), extraction of the encapsulated protein from the microspheres resulted in a larger dequenching effect at all time-points.

The encapsulated NIR-BSA recovered from the kidneys showed a gradual decline from 80 ± 11% directly after injection to around 10 ± 4% at day 21 post injection (Fig. 7A). The insert in Fig. 7A reflects the *in vivo* release of NIR-BSA from the microspheres and was calculated as 100 − percentage of the encapsulated NIR-BSA. It is more appropriate to calculate the *in vivo* release in such an indirect way than to derive it from the tissue levels of released NIR-BSA (supernatant I), since the released protein is subject to further redistribution and metabolism. As shown in Fig. 4C, with *in vitro* incubation of NIR-BSA-ms in phosphate buffer at 37 °C, 60% of the protein was released at day 35, as calculated with the BCA assay. In Fig. 7B, an *in vitro-in vivo* analysis was performed by plotting the percentage of the released NIR-BSA *in vitro* versus the percentage of NIR-BSA released *in vivo*. When comparing both *in vitro* and *in vivo* release, it is evident that protein release was faster *in vivo* with 89 ± 4% release within 2 weeks while 38 ± 1% was released *in vitro* in 2 weeks. In a previous study, we have shown that empty PLHMGA microspheres degraded *in vitro* within 35 days, which is in good agreement with the current *in vitro* degradation of NIR-BSA loaded microspheres [18]. The *in vivo* degradation of PLHMGA microspheres was also in good agreement albeit different detection methods were used. In this previous study, microspheres were not labeled and their presence in the tissue was mainly scored by visual recognition of their localization under the renal capsule. The current study enabled direct NIR detection of the intact microspheres at the early time points, and recovery of released and still encapsulated protein from the kidney homogenates at early and late time points. Therefore, while in both studies the intact microspheres were mostly gone in days 7–14 post injection due to erosion, the near-infrared signal was still detectable during the later stages of the experiment. Small microfragments of the eroded microspheres will not be pelletized as completely as intact microspheres in the extraction protocol as shown in Fig. 1, which will lead to an overestimation of the *in vivo* payload release rate in the present study. Nevertheless, a faster *in vivo* release of the payload from the injected microspheres compared to *in vitro* release was earlier reported by other authors, likely because *in vivo* hydrolytic enzymes contribute to the degradation of the particles [46–49].

Fig. 8 shows the renal levels of free NIR-BSA in the injected kidney homogenates calculated as the percentage of the injected dose. Of note, the effectuated levels of free NIR-BSA in the kidney result from the overall balance between the release rate and the local clearance of NIR-BSA in the kidney tissue. In the kidneys injected with NIR-BSA, the relative NIR-fluorescence decreased rapidly from 80 to 15% within the first 2 h after administration and around 10% of the dose was detected in this group at 24 h post injection. In kidneys injected with NIR-BSA-ms, an initial burst release of 14 ± 6% was seen, which is in agreement with the *in vitro* release data and the validation of the tissue extraction method as discussed above. The highest kidney levels of NIR-BSA were measured at day 3 post injection with 21 ± 5% of the injected dose. During the sustained release phase after injection of the depot, NIR-BSA tissue levels are mostly dependent on amount of protein released from the microspheres and the clearance of the NIR-BSA from the kidney tissue. Since no change is expected in the elimination mechanism of NIR-BSA during the course of the experiment, the observed peak level of NIR-BSA at day 3 indicates that this time-point corresponds to the highest release rate of the protein per time, which was equal to the protein being eliminated via the kidneys. Thereafter, a continuous fluorescent signal was seen in these kidneys until day 21

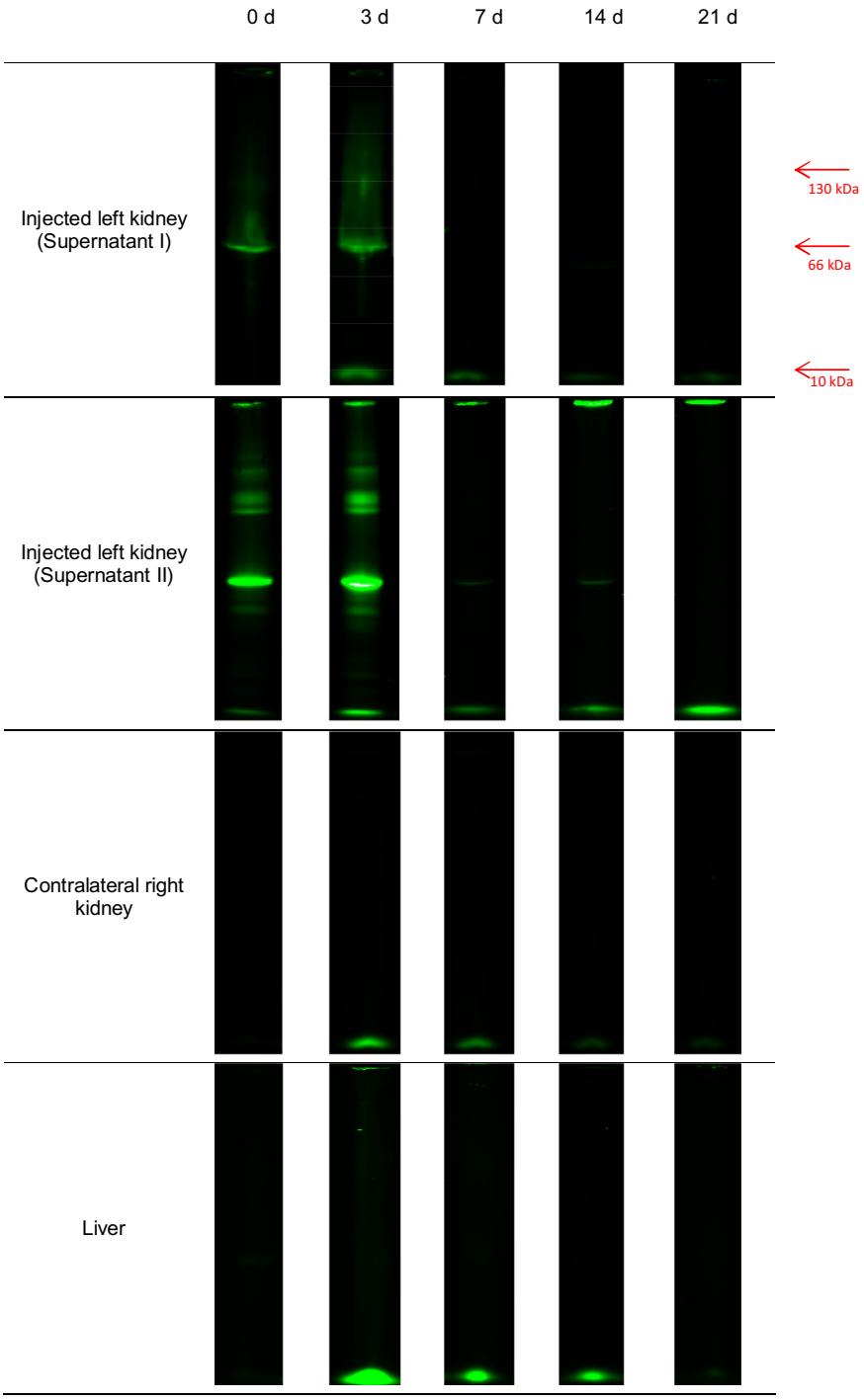

Fig. 12b. SDS–PAGE analysis of the organ homogenates from animals injected with NIR-BSA microspheres. The animals were sacrificed at day 0, 3, 7, 14 and 21 after injection. The homogenates of the injected left kidneys were treated as shown in Fig. 1A, where supernatant I represents the released protein from NIR-BSA microspheres and supernatant II is the signal measured from NIR-BSA after dissolving the microspheres. The low molecular weight compounds seen in the supernatant II are probably the degradation products of the NIR-BSA during liver metabolism, which are taken up by the kidneys, as also seen in the contralateral kidney, whereas the high molecular weight compounds that remain on the injection spot in the gel are probably caused by the extraction method.

post injection. The AUC of the free NIR-BSA in the kidneys, as calculated from Fig. 8, was six times higher for animals injected with NIR-BSA-ms (2440%·h; supernatant I; 0–7 days), compared to the AUC in the group injected with NIR-BSA (420% h; 0–24 h). This shows that the administration of NIR-BSA-ms resulted in prolonged tissue levels of NIR-BSA in the kidney compared to the injection of unencapsulated NIR-BSA.

3.4. Redistribution of NIR-BSA and metabolism

The organ distribution of NIR-BSA was assessed from the NIR-scanning of the explanted organs. Total organ relative NIR-signals of animals injected with NIR-BSA are shown in Fig. 9. The increased levels of NIR-BSA in the blood 2 h onwards demonstrate that the subcapsular injected protein redistributed from the

injection site into the circulation, where it subsequently accumulated mainly in the liver. The fluorescence signal showed high peak levels between 4 and 6 h post injection in all major organs, including the contralateral kidney (Fig. 9), which suggests that the degradation products are excreted from the circulation and undergo renal elimination. This is in agreement with other studies as well [41,45,50,51].

To determine whether the fluorescence was due to the intact NIR-BSA or to degradation products of NIR-BSA, homogenates and blood samples were subjected to SDS–PAGE separation after which the gels were scanned with the Odyssey NIR scanner (Figs. 10a and 10b). Intact NIR-BSA was detectable as a fluorescent band at 66 kDa, while protein degradation products were detected at the bottom of the gel (10 kDa). Blood (at 6 h) contained intact NIR-BSA, while NIR-fluorescence in the bladder originated from low-MW compounds (10 kDa), most likely NIR-BSA degradation products. Further discrimination was observed in tissues between the presence of intact NIR-BSA (the injected kidney at early time points) and NIR-BSA degradation products (in liver and other organs from 2 h and onwards). We postulate that intact NIR-BSA accumulates from the circulation in the liver while the enzymatically cleaved protein fragments are subsequently eliminated by the kidneys in urine. Previous studies with either the NIR dye or proteins labeled with this dye support the observed metabolic route of NIR-BSA [32,45,50,51]. Liver is known as the major organ for metabolizing albumin [52], where native albumin is taken up by the hepatocytes and degraded via lysosomes [53], whereas denaturated or chemically modified albumins are taken up by the liver macrophages (Kupffer cells) and are finally degraded in the lysosomes [54]. The degradation products are then known to be cleared by the kidneys [45].

In the group of animals injected with NIR-BSA-ms, organs were explanted at day 0, 3, 7, 14 and 21. Additional blood samples were drawn during the first 24 h and every second day, as described in Section 2.2.5. Similar to the group injected with NIR-BSA, a redistribution of the NIR-fluorescent signal was observed to the blood and the liver, although at a completely different time scale and intensities (Fig. 11). The above reported release of NIR-BSA in the kidney (Fig. 8), which peaked at day 3 post injection, coincided with the peak levels detected in liver and contralateral kidney (Fig. 11). Analysis of blood (Fig. 11B), however, showed an earlier peak with maximum NIR-fluorescence at 6 h, which coincides with the redistribution of NIR-BSA injected under the renal capsule (Fig. 9B). This makes it amenable that this early peak reflects initial burst-release of NIR-BSA from the injected microspheres. After day 7 post injection of NIR-BSA-ms, the levels of NIR-fluorescence in organs dropped to relatively low but still detectable values. At day 21 post injection NIR-fluorescence was still detectable in liver and contralateral kidney indicating that the depot was still releasing its cargo until the end of the experimental period (Fig. 11).

SDS–PAGE analysis of organ homogenates and blood samples from animals injected with NIR-BSA-ms are shown in Figs. 12a and 12b. Intact NIR-BSA protein was mainly detected in the blood sample and in the injected kidney. SDS–PAGE analysis of the extracted microspheres (Supernatant II) showed presence of monomeric NIR-BSA until day 14 post injection in the injected kidney, while liver, contralateral kidney and bladder homogenates mainly showed the presence of NIR-BSA degradation products of around 10 kDa. These low-molecular weight products represent the liver metabolites from NIR-BSA that undergo elimination through the kidneys. The presence of NIR-fluorescent degradation products in liver reflects that at least up to day 14, the microsphere depot has released its loaded cargo into the kidney from which it eventually redistributed to the circulation, while at day 21 hardly any NIR-BSA or NIR-BSA degradation products are detectable anymore in tissues.

4. Conclusion

In the present study, we demonstrate that protein loaded PLHMGA microspheres injected under the kidney capsule can serve as a depot of proteins, providing a continuous release at the site of administration over a period of 3 weeks. Additionally, the fluorescent signal remained the highest in the injected kidney at all time-points, while systemic levels remained very low. This approach therefore has the potential to reduce side effects of therapeutic proteins by increasing their presence at the site of injection and decreasing it elsewhere in the body. The use of the NIR dye in this study allows detection of low concentrations of the protein in tissue samples. We have also shown that the fluorescence signal detected in *ex vivo* images was not representative of true protein amounts as compared to measurements in tissue homogenates and thus requiring additional treatment of the samples. Cumulatively, this study shows an attractive delivery system of proteins into the kidney characterized by a longer release period and mainly local accumulation.

Acknowledgments/Disclosure

This research forms part of the Project P3.02 DESIRE of the research program of the BioMedical Materials institute, co-funded by the Dutch Ministry of Economic Affairs. The authors report no potential conflicts of interest.

Appendix A. Figures with essential color discrimination

Certain figures in this article, particularly Figs. 1–12, are difficult to interpret in black and white. The full color images can be found in the on-line version, at http://dx.doi.org/10.1016/j.actbio.2015.04.030).

References

[1] Star RA. Treatment of acute renal failure. Kidney Int 1998;54:1817–31.
[2] Silverstein DM. Inflammation in chronic kidney disease: role in the progression of renal and cardiovascular disease. Pediatr Nephrol 2009;24:1445–52.
[3] Kimmel PL et al. Immunologic function and survival in hemodialysis patients. Kidney Int 1998;54:236–44.
[4] Klahr S, Schreiner G, Ichikawa I. The progression of renal disease. N Engl J Med 1988;318:1657–66.
[5] Peppa M, Uribarri J, Cai W, Lu M, Vlassara H. Glycoxidation and inflammation in renal failure patients. Am J Kidney Dis 2004;43:690–5.
[6] Declèves AE, Sharma K. Novel targets of antifibrotic and anti-inflammatory treatment in CKD. Nat Rev Nephrol 2014;10:257–67.
[7] Arcasoy MO. The non-haematopoietic biological effects of erythropoietin. Br J Haematol 2008;141:14–31.
[8] Asadullah K, Sterry W, Volk HD. Interleukin-10 therapy – review of a new approach. Pharmacol Rev 2003;55:241–69.
[9] Yao Y et al. Interferon-γ improves renal interstitial fibrosis and decreases intrarenal vascular resistance of hydronephrosis in an animal model. Urology 2011;77:761.e8–761.e13.
[10] Zeisberg M. Bone morphogenic protein-7 and the kidney: current concepts and open questions. Nephrol Dial Transplant 2006;21:568–73.
[11] Tomlinson IM. Next-generation protein drugs. Nat Biotechnol 2004;22:521–2.
[12] Pisal DS, Kosloski MP, Balu-Iyer SV. Delivery of therapeutic proteins. J Pharm Sci 2010;99:2557–75.
[13] Tran VT, Benoit JP, Venier Julienne MC. Why and how to prepare biodegradable, monodispersed, polymeric microparticles in the filed of pharmacy? Int J Pharm 2011;407:1–11.
[14] Mitragotri S, Burke PA, Langer R. Overcoming the challenges in administering biopharmaceuticals: formulation and delivery strategies. Nat Rev Drug Discov 2014;13:655–72.
[15] Curtis LM, Chen S, Chen B, Agarwal A, Klug CA, Sanders PW. Contribution of intrarenal cells to cellular repair after acute kidney injury: subcapsular implantation technique. Am J Physiol Renal Physiol 2008;295:F310–4.
[16] Dankers PYW et al. Development and in-vivo characterization of supramolecular hydrogels for intrarenal drug delivery. Biomaterials 2012;33:5144–55.
[17] Dankers PYW et al. Hierarchical formation of supramolecular transient networks in water: a modular injectable delivery system. Adv Mater 2012;24:2703–9.

[18] Kazazi-Hyseni F et al. Biocompatibility of poly(D,L-lactic-co-hydroxymethyl glycolic acid) microspheres after subcutaneous and subcapsular renal injection. Int J Pharm 2015;482:99–109.
[19] Falke LL et al. Local therapeutic efficacy with reduced systemic side effects by rapamycin-loaded subcapsular microspheres. Biomaterials 2015;42:151–60.
[20] Ghassemi AH, Van Steenbergen MJ, Talsma H, Van Nostrum CF, Crommelin DJA, Hennink WE. Hydrophilic polyester microspheres: effect of molecular weight and copolymer composition on release of BSA. Pharm Res 2010;27:2008–17.
[21] Ghassemi AH et al. Preparation and characterization of protein loaded microspheres based on a hydroxylated aliphatic polyester, poly(lactic-co-hydroxymethyl glycolic acid). J Control Release 2009;138:57–63.
[22] Liu Y, Ghassemi AH, Hennink WE, Schwendeman SP. The microclimate pH in poly(D,L-lactide-co-hydroxymethyl glycolide) microspheres during biodegradation. Biomaterials 2012;33:7584–93.
[23] Seyednejad H, Ghassemi AH, van Nostrum CF, Vermonden T, Hennink WE. Functional aliphatic polyesters for biomedical and pharmaceutical applications. J Control Release 2011;152:168–76.
[24] Kazazi-Hyseni F et al. Computer modeling assisted design of monodisperse PLGA microspheres with controlled porosity affords zero order release of an encapsulated macromolecule for 3 months. Pharm Res 2014;31:2844–56.
[25] Nakashima T, Shimizu M, Kukizaki M. Membrane emulsification by microporous glass. Key Eng Mat 1991;61–62:513–6.
[26] Frangioni JV. In vivo near-infrared fluorescence imaging. Curr Opin Chem Biol 2003;7:626–34.
[27] Leemhuis M et al. Functionalized poly(a-hydroxy acid)s via ring-opening polymerization: toward hydrophilic polyesters with pendant hydroxyl groups. Macromolecules 2006;39:3500–8.
[28] Peters T. Serum albumin. In: Putman F, editor. The plasma proteins. New Delhi: Academic Press; 1975. p. 133–81.
[29] Nakashima T, Shimizu M, Kukizaki M. Particle control of emulsion by membrane emulsification and its applications. Adv Drug Deliv Rev 2000;45:47–56.
[30] Sah H. A new strategy to determine the actual protein content of poly(lactide-co-glycolide) microspheres. J Pharm Sci 1997;86:1315–8.
[31] Bjornsson OG, Murphy R, Chadwick VS, Bjornsson S. Physicochemical studies on indocyanine green: molar lineic absorbance, pH tolerance, activation energy and rate of decay in various solvents. J Clin Chem Clin Biochem 1983;21:453–8.
[32] Oliveira S et al. A novel method to quantify IRDye800CW fluorescent antibody probes ex vivo in tissue distribution studies. EJNMMI Res 2012;2:1–9.
[33] D'Aurizio E et al. Biodegradable microspheres loaded with an anti-Parkinson prodrug: an in vivo pharmacokinetic study. Mol Pharm 2011;8:2408–15.
[34] Schliecker G, Schmidt C, Fuchs S, Ehinger A, Sandow J, Kissel T. In vitro and in vivo correlation of buserelin release from biodegradable implants using statistical moment analysis. J Control Release 2004;94:25–37.
[35] Ghassemi AH et al. Preparation and characterization of protein loaded microspheres based on a hydroxylated aliphatic polyester, poly(lactic-co-hydroxymethyl glycolic acid). J Control Release 2009;138:57–63.
[36] Samadi N, Van Nostrum CF, Vermonden T, Amidi M, Hennink WE. Mechanistic studies on the degradation and protein release characteristics of poly(lactic-co-glycolic-co-hydroxymethylglycolic acid) nanospheres. Biomacromolecules 2013;14:1044–53.
[37] Heuveling DA et al. Nanocolloidal albumin-IRDye 800CW: a near-infrared fluorescent tracer with optimal retention in the sentinel lymph node. Eur J Nucl Med Mol Imaging 2012;39:1161–8.
[38] Leblond F, Davis SC, Valdes PA, Pogue BW. Pre-clinical whole-body fluorescence imaging: review of instruments, methods and applications. J Photochem Photobiol B 2010;98:77–94.
[39] Durand E, Chaumet-Riffaud P, Grenier N. Functional renal imaging: new trends in radiology and nuclear medicine. Semin Nucl Med 2011;41:61–72.
[40] Gross S, Piwnica-Worms D. Molecular imaging strategies for drug discovery and development. Curr Opin Chem Biol 2006;10:334–42.
[41] Oliveira S et al. Rapid visualization of human tumor xenografts through optical imaging with a near-infrared fluorescent anti-epidermal growth factor receptor nanobody. Mol Imaging 2012;11:33–46.
[42] Kunjachan S, Gremse F, Theek B, Koczera P, Pola R, Pechar M, et al. Noninvasive optical imaging of nanomedicine biodistribution. ACS Nano 2013;7:252–62.
[43] Hou Y, Liu Y, Chen Z, Gu N, Wang J. Manufacture of IRDye800CW-coupled Fe_3O_4 nanoparticles and their applications in cell labeling and in vivo imaging. J Nanobiotechnol 2010;8:25.
[44] Eker OF et al. Combination of cell delivery and thermoinducible transcription for in vivo spatiotemporal control of gene expression: a feasibility study. Radiology 2011;258:496–504.
[45] Vasquez KO, Casavant C, Peterson JD. Quantitative whole body biodistribution of fluorescent-labeled agents by non-invasive tomographic imaging. PLoS ONE 2011;6.
[46] Wöhl-Bruhn S et al. Comparison of in vitro and in vivo protein release from hydrogel systems. J Control Release 2012;162:127–33.
[47] Van Apeldoorn AA, Van Manen HJ, Bezemer JM, De Bruijn JD, Van Blitterswijk CA, Otto C. Raman imaging of PLGA microsphere degradation inside macrophages. J Am Chem Soc 2004;126:13226–7.
[48] Walter E et al. Hydrophilic poly(DL-lactide-co-glycolide) microspheres for the delivery of DNA to human-derived macrophages and dendritic cells. J Control Release 2001;76:149–68.
[49] Jiang G, Woo BH, Kang F, Singh J, DeLuca PP. Assessment of protein release kinetics, stability and protein polymer interaction of lysozyme encapsulated poly(D,L-lactide-co-glycolide) microspheres. J Control Release 2002;79:137–45.
[50] Marshall MV, Draney D, Sevick-Muraca EM, Olive DM. Single-dose intravenous toxicity study of IRDye 800CW in sprague-dawley Rats. Mol Imaging Biol 2010;12:583–94.
[51] Tanaka E, Ohnishi S, Laurence RG, Choi HS, Humblet V, Frangioni JV. Real-time intraoperative ureteral guidance using invisible near-infrared fluorescence. J Urol 2007;178:2197–202.
[52] Rothschild MA, Oratz M, Schreiber SS. Regulation of albumin metabolism. Annu Rev Med 1975;26:91–104.
[53] Ohshita T, Hiroi Y. Degradation of serum albumin by rat liver and kidney lysosomes. J Nutr Sci Vitaminol (Tokyo) 1998;44:641–53.
[54] Nilsson M, Berg T. Uptake and degradation of formaldehyde-treated 125I-labelled human serum albumin in rat liver cells in vivo and in vitro. Biochim Biophys Acta 1977;497:171–82.